

1 Evaluation of machine learning methods for organic apple authentication  
2 based on diffraction grating and image processing

3 Weiran Song <sup>a</sup>, Nanfeng Jiang <sup>b, \*</sup>, Hui Wang <sup>a</sup>, Gongde Guo <sup>b</sup>

4 <sup>a</sup> *School of Computing, Ulster University, BT37 0QB, Newtownabbey, Co. Antrim, UK*

5 <sup>b</sup> *School of Mathematics and Informatics, Fujian Normal University, 350007, Fuzhou, China*

6 \* Corresponding author.

7 *E-mail address: [jiangbbplayer@163.com](mailto:jiangbbplayer@163.com) (N. Jiang).*

8 **Abstract**

9 Optical measuring technologies coupled with machine learning algorithms can be used to build a home-made  
10 sensor system. We built such a sensor system using a smartphone and a diffraction grating sheet. Diffraction  
11 images were captured under white light illumination and converted into a data matrix for data analysis. In  
12 this paper we present a systematic evaluation of this sensor system on the task of differentiating organic  
13 apples from conventional ones. We used the sensor system to measure 150 organic and conventional apples  
14 as rainbow images. We processed the rainbow images using computer vision techniques, built machine  
15 learning and chemometrics models, and used the resultant models to classify testing samples. Moreover, a  
16 comparative study was conducted where the same set of apples were scanned by a commercial spectrometer  
17 resulting in spectral data of the apple samples and classification was undertaken using partial least squares  
18 discriminant analysis (PLS-DA). Experimental results show that state of the art machine learning algorithms  
19 such as support vector machine (SVM) and locally weighted partial least squares classifier (LW-PLSC) are  
20 effective in handling low-quality image data with classification accuracies of 93–100%. These results suggest  
21 that the sensor system is convenient and low-cost, and provides a fast, effective, non-destructive and viable  
22 solution for in-line food authentication.

23 *Keywords:* Food authentication, Organic apple, Diffraction grating, Machine learning, Chemometrics

## 24 **1. Introduction**

25 Apple, which plays an important role in healthy diet, is one of the most cultivated and consumed fruits in  
26 the world. According to FAOSTAT, the total apple production reached 83.1 million tons worldwide in 2017  
27 (<http://www.fao.org/faostat>). Meanwhile, apple quality is gaining increasing attention due to the rising  
28 concerns about food safety and quality. Some issues related to the external and internal quality of apple, such  
29 as bruise degree, diseases, pesticide residue contamination and organic fraud, pose a serious threat to  
30 consumer health and damage the fair trade-off between quality and price. Traditional testing techniques based  
31 on sensory and chemical analysis are laborious and time-consuming, so they do not meet the growing demand  
32 for large-scale and real-time apple quality testing in industrial process and consumer market.

33 Optical sensors coupled with chemometrics have become an effective approach to predict the quantitative  
34 and qualitative attributes of apple (Ignat et al., 2014; Moscetti et al., 2018). They are also effective for rapid  
35 and non-invasive food evaluation which requires minimal sample preparations. For quantitative research,  
36 many studies investigate the internal contents of apples by using near-infrared (NIR) spectroscopy and NIR  
37 hyperspectral imaging techniques. These studies predict the internal contents, including sweetness (soluble  
38 solids content, SSC) (Ma et al., 2018; Tang et al., 2018; Yuan et al., 2016), sourness (acidity or pH value)  
39 (Ignat et al., 2014; Jha and Ruchi, 2010), firmness (Ignat et al., 2014) and moisture (Dong and Guo, 2015),  
40 which directly influence flavours and textures of apples. Other studies are related to food safety and health  
41 issues, i.e., the pesticide contamination of apples. It has been reported that surface-enhanced Raman  
42 spectroscopy (SERS), Fourier transform infrared (FTIR) spectroscopy and laser-induced breakdown  
43 spectroscopy (LIBS) techniques can effectively measure the level of pesticide residuals on apple surface,  
44 such as chlorpyrifos (Dhakal et al., 2014; Ma and Dong, 2014; Xiao et al., 2015), carbaryl (Fan et al., 2015),  
45 phosmet and thiabendazole (Luo et al., 2016). Spectroscopy and hyperspectral imaging are also two state of  
46 the art techniques for determining apple qualities, for example, identifying varieties, grades, geographical  
47 origins (Luo et al., 2011), detecting apple diseases (Jarolmasjed et al., 2017) and bruising degree (Tan et al.,  
48 2018; Vetrekar et al., 2015). Furthermore, computer vision system (CVS) is recently used for the evaluation  
49 of ripening stages (Cárdenas-Pérez et al., 2017), surface gloss (Sun et al., 2017), diseases (Dubey and Jalal,  
50 2016) and defectiveness (Zhang et al., 2015).

51 The use of portable spectrometer for real-time apple **quality assessment** is in a strong uptrend which has  
52 met the requirement for practical use (Gao et al., 2016; Yuan et al., 2016). **Our previous studies have**  
53 **demonstrated that the use of portable NIR spectrometer coupled with chemometrics provides a feasible**  
54 **approach for authenticating organic apples with an accuracy of over 90% (Song et al., 2018a, 2016). This**  
55 **approach is simple, quick and non-destructive compared to conventional analytical techniques for**  
56 **authenticating organic foods such as compound-specific isotope analysis (CSIA), inductively coupled**  
57 **plasma-mass spectrometry (ICP-MS), isotope ratio mass spectrometry (IRMS) (de Lima and Barbosa, 2019).**  
58 **However, the miniaturisation and field portability of spectrometers** will normally degrade the fingerprint data  
59 quality due to the variable sampling conditions, posing challenges to linear chemometric algorithms (Liu et  
60 al., 2018; Song et al., 2018a). One of the most standard chemometric method for data classification is partial  
61 least squares discriminant analysis (PLS-DA), which effectively handles high dimensionality, high  
62 collinearity and small sample size problems. However, it sometimes yields unsatisfied performance due to  
63 the high degree of nonlinearity (Song et al., 2018b; Zou et al., 2010). To tackle this issue, many machine  
64 learning algorithms have been investigated and become an indispensable part in chemometrics field. For  
65 example, nonlinear classifiers such as support vector machine (SVM) and random forest (RF) are often well-  
66 performing in classifying spectral data due to the good generalization performance (Devos et al., 2009; Zhang  
67 et al., 2016). Artificial neural networks (ANN) and extreme learning machine (ELM) can also efficiently  
68 capture the nonlinear relationship between observations and classes, gaining an advantage over PLS-DA in  
69 classification accuracy and robustness (Moncayo et al., 2015; Zheng et al., 2014).

70 Despite the fact that nonlinear algorithms can improve the classification capability of low-quality spectral  
71 data to some extent, the price of portable spectrometer far exceeds expectation in consumer market. Recent  
72 studies attempt to use CVS for food quality evaluation based on mobile devices such as smartphone and  
73 tablet (Cruz-Fernández et al., 2017; Cubero et al., 2018), which demonstrate potential in on-line application.  
74 CVS simulates human visual system using artificial sensor and automatically gains high-level understanding  
75 from digital images via image acquisition, processing and data analysis. Our recent study proposes a low-  
76 cost CVS based on diffraction grating and demonstrates its feasibility in organic apple identification (Jiang  
77 et al., 2018). This study uses locally weighted partial least squares classifier (LW-PLSC) to handle nonlinear

78 food data which significantly improves the classification performance compared to PLS-DA. Nevertheless,  
79 an up-to-date comparative study is essential for three reasons: first, LW-PLSC requires to be evaluated by  
80 comparing its capability with baseline classifiers; second, the empirical reference in selecting the most  
81 appropriate classifiers for the new type of image data has yet been studied; third, the performance comparison  
82 between the new sensor system and the other optical sensors such as spectrometer remains to be investigated.

83 **Organic apples are generally more expensive than conventional ones. This, coupled with the fact that**  
84 **visual differentiation between organic and conventional apples is often not possible, has led to organic food**  
85 **fraud involving apples.** In this study, we aim to distinguish organic and conventional labelled apples using a  
86 combination of low-cost sensor system and supervised machine learning methods. We evaluate the  
87 classification performance of ten methods on rainbow image data, including PLS-DA, kernel PLS-DA  
88 (KPLS-DA), LW-PLSC, soft independent modelling of class analogies (SIMCA),  $k$ -nearest neighbours ( $k$ -  
89 NN), logistic regression (LR), SVM, least squares SVM (LS-SVM), decision tree (C4.5) and RF, and choose  
90 the best-performing ones under different sample distributions. Then a benchmark instrument, a commercial  
91 high-resolution spectrometer, is used to measure the same samples and compared with the sensor system in  
92 identifying organic and conventional apples. This study reveals that the low-quality image data obtained from  
93 low-cost measurement is effective for apple fruit authentication with the aid of high performance machine  
94 learning methods.

## 95 **2. Materials and methods**

### 96 *2.1. Sample preparation*

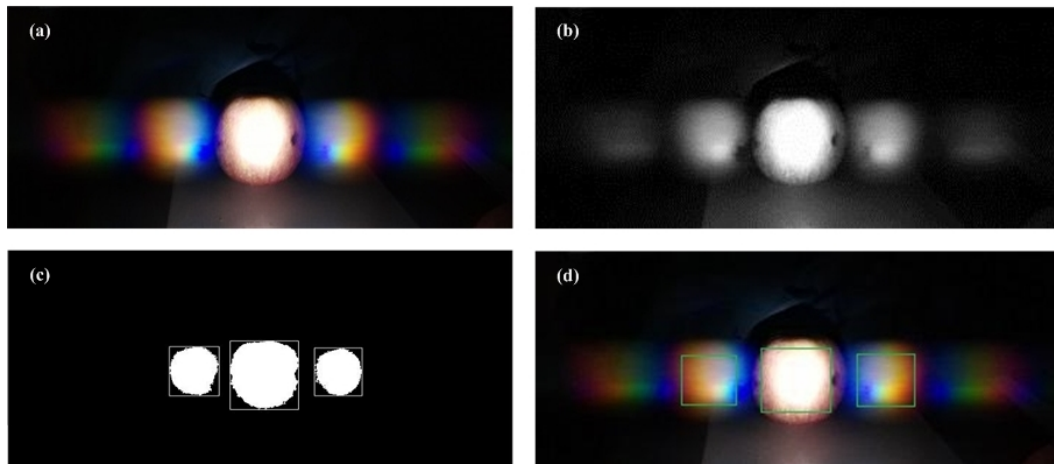
97 A total of 150 apples were collected from local super markets in Fuzhou during a week. **There were three**  
98 **apple varieties (50 Braeburn, 50 Gala and 50 Pink lady, respectively) and each variety contained two classes**  
99 **(25 organic and 25 conventional, respectively).** All apples were defect-free, similar in size and maturity, and  
100 no surface preparation was carried out prior to data collection. We conducted the imaging and spectral  
101 measurements at room temperature ( $22 \pm 2$  °C).

102 2.2. *Imaging system based on diffraction grating*

103 A recently proposed sensor system is used to obtain image data from apple samples, which includes  
104 diffraction image acquisition, rainbow image extraction and feature vector representation (Jiang et al., 2018).

105 2.2.1. *Diffraction image acquisition*

106 An apple sample was placed 20 cm in front of a flashlight, two diffraction grating sheet ( $60 \times 40$  nm) was  
107 set on both sides of the apple and a smartphone camera was fixed by 1 cm above the flashlight. We use the  
108 flashlight to illuminate the apple surface, so reflected polychromatic light can pass through a diffraction  
109 grating and then disperse into several beams travelling in different directions. Each beam has a single rainbow  
110 of colours under white light illumination. Then the rainbows are photographed by smartphone with  $1080 \times$   
111  $720$  pixels spatial resolution and stored in JPG format with file size of approximately 1.14MB. To eliminate  
112 the influence of ambient light and generate comparably high-quality data, the image acquisition was  
113 conducted in a dark environment. Fig. 1a shows a central part of the diffraction image with rainbow colour  
114 spectra.



115

116

117

**Fig. 1.** (a) The original diffraction image of rainbow colour spectra; (b) grayscale processed image; (c) mathematical morphology processed image; (d) the extracted rainbows in image.

118 2.2.2. *Rainbow image extraction*

119 We use a combination of image processing techniques to extract a single rainbow from the obtained  
120 diffraction image, including pre-processing, denoising and segmentation. Grayscale processing firstly converts  
121 colour pixels into grey ones (see Fig. 1b) which only carry intensity information. This step enables  
122 mathematical morphology to capture the most essential shape features of target rainbows, as shown in Fig.  
123 1c. Then denoising adopts median filter to replace the value of a point in the digital image with the median  
124 of neighbouring points. Finally, the OSTU method (Otsu, 1979) calculates the foreground and background  
125 class probability, so a single rainbow image can be derived from the raw diffraction image (see Fig. 1d). A  
126 resized rainbow image ( $50 \times 100$  pixels) to be converted into numerical values is shown Fig. 2.



127  
128

**Fig. 2.** The resized rainbow image ( $50 \times 100$  pixels) of an apple sample.

129 2.2.3. *Feature vector representation*

130 We map the rainbow image into 3-dimensional Cartesian coordinate system of red (R), green (G) and  
131 blue (B) colour. Each colour channel has 256 colour levels varying from 0 to 255. It is noted that the row  
132 pixels usually contain more hues than the column pixels, so we calculate the mean of each column and use  
133 the obtained feature vector to represent the spectral line of sample. The raw image data is shown in Fig. 3.

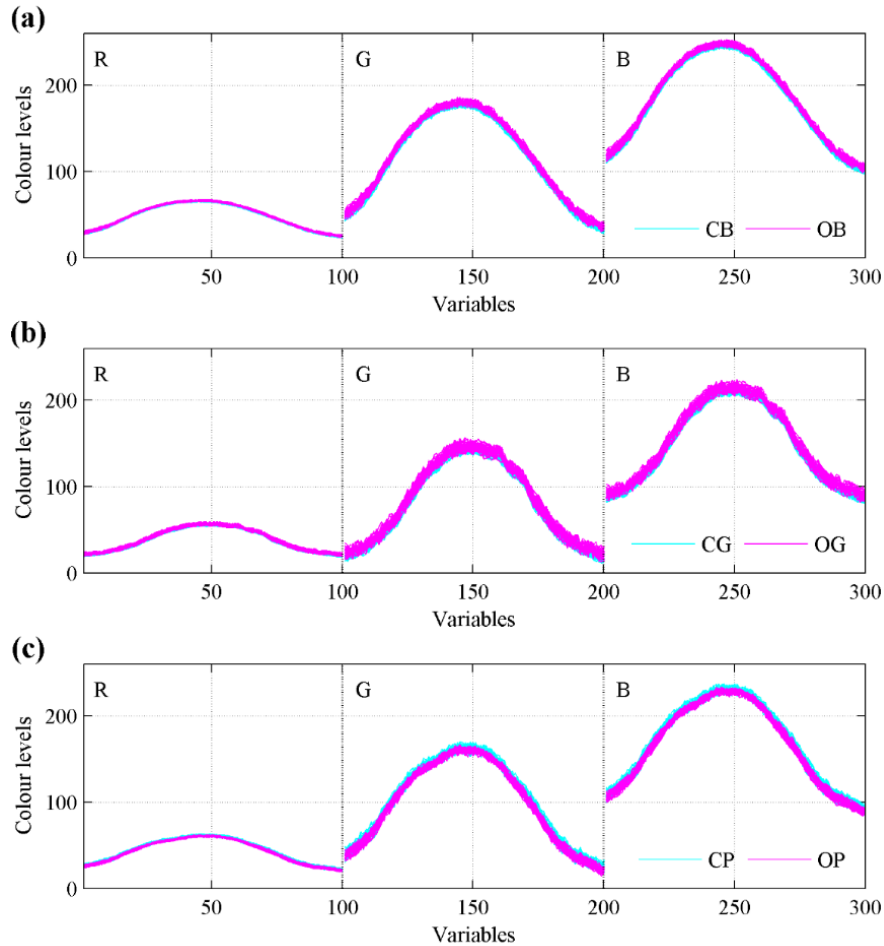
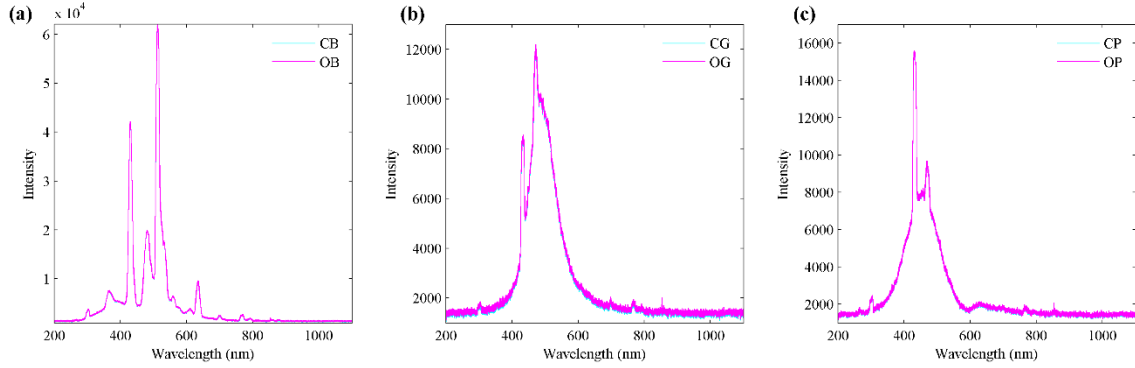


**Fig. 3.** The raw image data of Braeburn (B), Gala (G) and Pink lady (P) apples. Data in cyan and magenta colour represents conventional (C) and organic (O) samples, respectively. Variables 1-100, 101-200 and 201-300 belongs to red, green and blue channels, respectively.

134  
135  
136  
137

### 138 2.3. Spectroscopy

139 Apples spectral reflectance data were collected with a high-resolution spectrometer (USB4000-FL  
140 spectrometer, Ocean Optics, Inc., USA) equipped with an optical fiber probe and having a wavelength range  
141 of 200-1100 nm with an interval of 0.9879 nm. The experiments were conducted under ambient light  
142 conditions in a colour assessment cabinet which can provide a standard visible light source. Apple spectra of  
143 three varieties were collected with the Ocean-View software containing 912 variables, as shown in Fig. 4.



144  
 145 **Fig. 4.** Conventional and organic apple spectra (148 samples and 912 variables) of three varieties (Braeburn, Gala and Pink lady). Two  
 146 outliers in Gala and Pink lady varieties have been removed for better visualization.

147 *2.4. Data analysis*

148 *2.4.1. Sample division and pre-processing*

149 As the investigated apples contain six groups, namely, conventional Braeburn (CB), organic Braeburn  
 150 (OB), conventional Gala (CG), organic Gala (OG), conventional Pink lady (CP) and organic Pink lady (OP),  
 151 we use DUPLEX algorithm (Snee, 1977) to partition apples belonging to the same group into training and  
 152 testing samples according to the ratio of 2:1. To explore the differentiation between conventional and organic  
 153 apples within each variety, training samples belongs to CB and OB groups are merged as a whole training  
 154 set for Braeburn variety meanwhile the corresponding testing samples are combined as a testing set. The  
 155 same procedure is also applied on Gala and Pink lady varieties. We also attempt to build models based on  
 156 the overall varieties and classify testing samples of different varieties. Therefore, we integrate the three  
 157 training sets and mix the corresponding testing sets. Such way of sample division maintains the same diversity  
 158 in both sets and keeps the balance between two classes.

159 We only apply Savitzky-Golay smoothing (fitted by a polynomial of degree two and a 33-point moving  
 160 window) to pre-process raw image data, because our previous study reports such pre-processing can  
 161 effectively reduce the noise and improves the modelling performance (Jiang et al., 2018). For data obtained  
 162 from spectroscopy, we use raw spectra without pre-processing due to its high quality and the high  
 163 performance of PLS-DA. This will be demonstrated in Section 3.



164 2.4.2. Classification methods

165 This work implements ten commonly used algorithms in chemometrics and machine learning fields to  
166 classify apple image data. PLS-DA relies on the assumption that the investigated system or process is driven  
167 by a set of latent variables (LVs) in low dimensional space. It transforms the categorical vector into numerical  
168 responses and searches for latent variables with maximum covariance with the responses (Barker and Rayens,  
169 2003). KPLS-DA maps the original data into Hilbert feature space via kernel function and then constructs a  
170 PLS-DA model for classification. The nonlinear relationship among variables in the original sample space  
171 becomes linear after mapping, so data nonlinearity can be effectively captured. LW-PLSC is an extension of  
172 LW-PLS (Kim et al., 2011), which uses weighting schemes for queries which respectively enlarges and  
173 lessens the influence of neighbouring and remote samples towards a PLS-DA model. Thus, the degree of  
174 global nonlinearity is reduced by using local linear models. SIMCA performs PCA on each class and  
175 constructs principal component models with the optimal numbers of PCs identified by cross-validation. A  
176 query is then attributed to the class which yields the least residue during prediction.

177 The  $k$ -NN predicts a query according to the  $k$  closest samples of the query and assign it to the class which  
178 has the largest category probability. The Euclidean distance is the most commonly used distance function in  
179  $k$ -NN, however, it can barely provide sufficient distinctions between different samples in high-dimensional  
180 case (Aggarwal et al., 2001). The LR is a widely used statistical model which aims to solve binary  
181 classification problems. It extends ordinary least squares to model the logistic relationship between the  
182 probability of class membership and the input variables. The SVM classification searches for a hyperplane  
183 to correctly separate samples of different classes meanwhile maximizing the shortest distances from the  
184 hyperplane to the nearest samples for each class. It can be extended to non-linear classification by projecting  
185 data from low dimensional input space to high dimensional feature space via kernel functions. The LS-SVM  
186 is an advanced version of SVM for binary classification which applies the linear least squares criteria to the  
187 loss function instead of inequality constraints (Suykens and Vandewalle, 1999). Decision tree uses a  
188 flowchart-like structure to present the various outcomes from a series of decisions. It mainly consists of a  
189 root node, branches and leaf nodes. The root node represents a query to be assigned, the branch represents  
190 the flow from question to answer and the leaf node represents a class label. The RF is an ensemble method

191 **which** generates multiple decision trees and predict a query based on a simple majority voting of the single  
192 classification tree.

193 In our experiments, the decision tree classifier (C4.5) was from the WEKA learning environment using  
194 J48 function while other classifiers were from MATLAB (Mathworks, 2011a). Some baseline classifiers  
195 were from MATLAB external toolboxes, including LIBSVM toolbox (SVM) (Chang and Lin, 2011),  
196 Classification toolbox (SIMCA) (Ballabio and Consonni, 2013) and LS-SVM toolbox (LS-SVM) (De  
197 Brabanter et al., 2011).

#### 198 2.4.3. Parameter setting

199 We use leave-one-out cross validation on training set to optimize the parameters of different algorithms.  
200 The range of LVs in PLS-DA, KPLS-DA and LW-PLSC is set from 1 and 10 to prevent overfitting. The  
201 number of components for each class model in SIMCA is no more than 10. The number of nearest neighbours  
202 in  $k$ -NN is selected from 1 to 15. The regularization parameter  $\lambda$  in LR is varied from  $10^{-7}$  to  $10^3$  on a  
203 logarithmic scale. This work adopts radial basis function for three kernel methods and implements a grid  
204 search approach for kernel methods and LW-PLSC. The width of the RBF  $\sigma$  in KPLS-DA are 1, 5, 10, 50,  
205 100, 500 and 1000. The regularization parameter  $C$  ( $C = 1, 10, 100, 1000$ ) and RBF kernel parameter  $\gamma$  ( $\gamma =$   
206  $10^{-5}, 5 \times 10^{-5}, 10^{-4}, 5 \times 10^{-4}, 10^{-3}, 5 \times 10^{-3}, 10^{-2}$ ) totally construct 28 SVM models, while the parameters of LS-  
207 SVM build 20 models ( $C = 1, 10, 100, 1000$  and  $\sigma = 1, 10, 100, 1000, 10000$ ). The localization parameter  $\varphi$   
208 in LW-PLSC is adjusted to the values of 0.1, 0.5, 1, 5, 10, 15 and 20. The depth of tree in C4.5 are 2, 4, 6, 8,  
209 10, 12 and 14. We use the default setting of RF parameters ( $n_{tree} = 500$ ,  $m_{try} = \sqrt{p}$  and  $nodesize = 1$ , where  
210  $p$  is the number of variables) for validation and classification, which has been reported well-performing in  
211 most cases (Strobl et al., 2009).

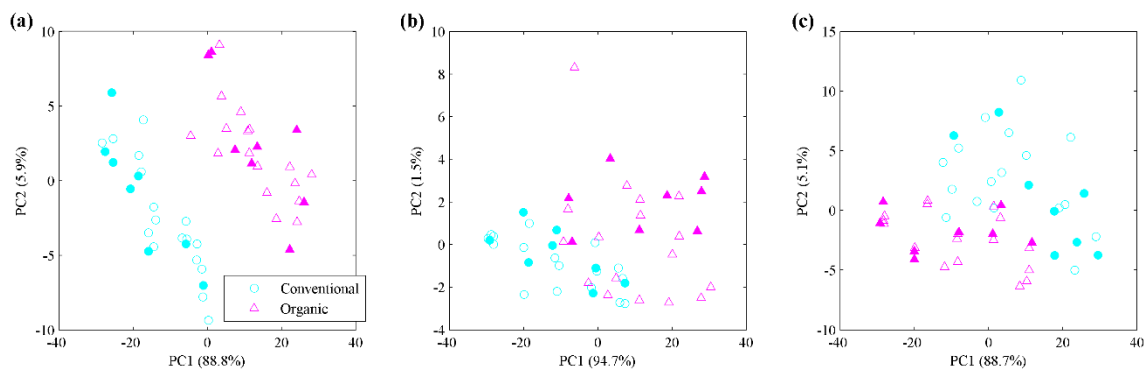
### 212 3. Results and discussion

#### 213 3.1. PCA of image and spectral data

214 The data of each apple variety plotted according to the PCA scores is shown in Fig. 5. Training and testing  
215 data are represented as empty and filled points, respectively. The first two principal components (PCs)

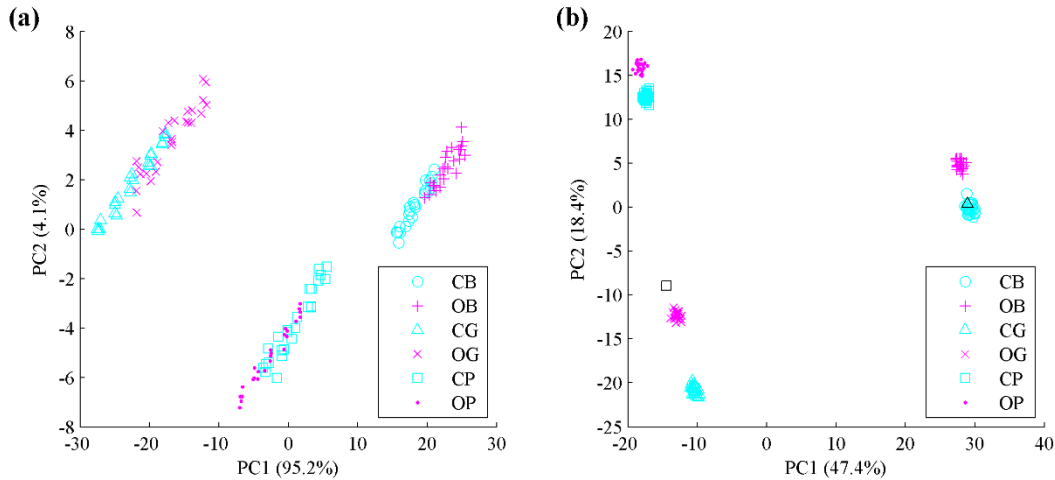
216 accumulate over 93% of the total variance in each variety. Samples of Braeburn variety have a good  
217 separation between organic and conventional classes, while samples of Gala or Pink lady varieties present an  
218 overlap between two classes. Reasonable classification models may exist in Gala and Pink lady varieties  
219 despite the visualized two dimensions does not display a clear separation.

220 The PCA charts of the overall samples obtained from imaging and spectroscopy are shown in Fig. 6a and  
221 b, respectively. The distinction of samples based on apple varieties is quite clear compared to that of samples  
222 based on classes. Data obtained from low-cost imaging technique fails to provide a linear separation between  
223 organic and conventional classes by using two PCs, while data collected by high-resolution spectroscopy  
224 presents a good class separation. Typically, spectral data of individual variety are linearly separable based on  
225 organic and conventional classes. Two outliers from CG and CP groups can be identified from the PCA  
226 scatter plot of spectral data, which may be induced by mislabelling or measuring distortion.



227  
228  
229

**Fig. 5.** PCA scatter plot of rainbow image data: Braeburn (a), Gala (b) and Pink lady (c) apples. Training and testing data are represented as empty and filled points, respectively.



230  
 231 **Fig. 6.** PCA scatter plots of the apple data from imaging (a) and spectroscopy (b). CB: conventional Braeburn; OB: organic Braeburn;  
 232 CG: conventional Gala; OG: organic Gala; CP: conventional Pink lady; OP: organic Pink lady. Two outliers from CG and CP group  
 233 are marked as black in spectral data.

234 *3.2. Classification of image and spectral data*

235 The classification of apple image datasets, including each variety and the overall varieties, are presented  
 236 in Table 1 and

237 Table 2. For Braeburn variety, despite several algorithms (LR, *k*-NN, C4.5 and RF) misclassify one  
 238 sample in training phase, all algorithms can successfully identify testing samples. For Gala variety, both  
 239 KPLS-DA and SVM reach the highest results of 94.1% and 100%, respectively in training and testing phase.  
 240 Moreover, LW-PLSC and LS-SVM have the same results of 100% in classification. While other classifiers  
 241 yield lower validation and classification results ranging from 76.5% (SIMCA and *k*-NN) to 91.2% (LS-SVM)  
 242 and 75% (SIMCA) to 93.8% (PLS-DA, LR and *k*-NN), respectively. The number of wrongly classified  
 243 organic apples does not exceed 1 for most of the algorithms. For Pink lady variety, the highest validation  
 244 accuracy is 91.2% obtained by KPLS-DA, while that of classification is 100% achieved by both KPLS-DA  
 245 and *k*-NN. Other classifiers yield lower validation and classification results which are respectively below  
 246 90% and 95%. The conventional samples are easily identified by all algorithms, while the organic ones can  
 247 only be correctly recognised by KPLS-DA and *k*-NN. The highest accuracy of the overall dataset is lower  
 248 than that of each dataset. LW-PLSC and RF models attain the highest validation results of 90.2% while LW-  
 249 PLSC and *k*-NN give the best performance in classification with 97.9% accuracy. Classifiers such as KPLS-

250 DA, SVM and LS-SVM provide comparable results in both phases. The highest accuracy of organic class  
 251 (95.8%) is obtained by LW-PLSC, SIMCA and  $k$ -NN, of which 23 out of 24 samples are correctly identified.

252 Table 1

253 The accuracy (%) of different algorithms for the classification of organic and conventional apples (Braeburn and Gala varieties) based  
 254 on data obtained from diffraction images.

Braeburn	Training	Testing	Organic	Conventional	Gala	Training	Testing	Organic	Conventional
PLS-DA	<b>100</b>	<b>100</b>	100	100	PLS-DA	85.3	93.8	87.5	100
KPLS-DA	<b>100</b>	<b>100</b>	100	100	KPLS-DA	<b>94.1</b>	<b>100</b>	100	100
LW-PLSC	<b>100</b>	<b>100</b>	100	100	LW-PLSC	88.2	<b>100</b>	100	100
SVM	<b>100</b>	<b>100</b>	100	100	SVM	<b>94.1</b>	<b>100</b>	100	100
LS-SVM	<b>100</b>	<b>100</b>	100	100	LS-SVM	91.2	<b>100</b>	100	100
SIMCA	<b>100</b>	<b>100</b>	100	100	SIMCA	76.5	75	100	50
LR	97.1	<b>100</b>	100	100	LR	82.4	93.8	87.5	100
$k$ -NN	97.1	<b>100</b>	100	100	$k$ -NN	76.5	93.8	87.5	100
C4.5	97.1	<b>100</b>	100	100	C4.5	85.3	87.5	87.5	87.5
RF	97.1	<b>100</b>	100	100	RF	85.3	81.3	75	87.5

255

256 Table 2

257 The accuracy (%) of different algorithms for the classification of organic and conventional apples (Pink lady and the overall varieties)  
 258 based on data obtained from diffraction images.

Pink lady	Training	Testing	Organic	Conventional	Overall	Training	Testing	Organic	Conventional
PLS-DA	85.3	93.8	87.5	100	PLS-DA	55.9	58.3	58.3	58.3
KPLS-DA	<b>91.2</b>	<b>100</b>	100	100	KPLS-DA	89.2	95.8	91.7	100
LW-PLSC	88.2	93.8	87.5	100	LW-PLSC	<b>90.2</b>	<b>97.9</b>	95.8	100
SVM	88.2	93.8	87.5	100	SVM	88.2	95.8	91.7	100
LS-SVM	88.2	93.8	87.5	100	LS-SVM	89.2	95.8	91.7	100
SIMCA	85.3	87.5	75	100	SIMCA	70.6	79.2	95.8	62.5
LR	85.3	93.8	87.5	100	LR	58.8	60.4	54.2	66.7
$k$ -NN	85.3	<b>100</b>	100	100	$k$ -NN	86.3	<b>97.9</b>	95.8	100
C4.5	76.5	93.8	87.5	100	C4.5	84.3	87.5	75	100
RF	82.4	93.8	87.5	100	RF	<b>90.2</b>	93.8	91.7	95.8

259 Among the ten algorithms, KPLS-DA achieves the top validation and classification results on the first  
 260 three datasets. SVM based algorithms also present good classification performance on four datasets.  
 261 Nevertheless, kernel method is more prone to overfitting than its non-kernel counterpart if data has a limited  
 262 number of samples (Despaigne et al., 2000). By adjusting the contribution of training samples in a local model  
 263 for a query, LW-PLS classification improves the performance of PLS-DA on the classification of nonlinear  
 264 data. Linear classifiers i.e., PLS-DA and LR, provide acceptable results for differentiating organic apples

265 from conventional ones within each variety. However, such results will drastically degrade by over 30%  
 266 when classifying testing samples from the overall varieties. The  $k$ -NN provides the highest classification  
 267 accuracies in three datasets by selecting one nearest neighbour. However, the validation results of  $k$ -NN are  
 268 usually lower than that of kernel algorithms.

269 We also provide the validation and classification results of PLS-DA on apple spectral datasets, as in  
 270 **Error! Not a valid bookmark self-reference.. PLS-DA model can effectively identify organic samples in**  
 271 **Braeburn, Gala and Pink lady varieties with validation results of 100%, 97.1% and 97.1%, respectively.** Two  
 272 outliers from CG and CP groups are the only misclassified samples. However, the outlier from CG group can  
 273 be correctly attributed to the conventional class as it is close to CB samples in PCA scatter plot (see Fig. 6b),  
 274 **yielding an overall accuracy of 99% in validation.** PLS-DA selects additional numbers of LVs across the  
 275 overall dataset, showing an increased degree of nonlinearity. Nevertheless, the optimal number of LVs  
 276 identified by leave-one-out cross validation does not exceed 3 for each dataset. The corresponding PLS-DA  
 277 model has low simplicity but still **correctly distinguish organic apples from conventional ones on the four**  
 278 **datasets** due to the high quality of spectral data.

279 Table 3

280 **The accuracy (%) of PLS-DA for the classification of organic and conventional apples (Braeburn, Gala, Pink lady and the overall**  
 281 **varieties) based on data obtained from spectroscopy.**

Datasets	Training	LVs	Testing	Organic	Conventional
Braeburn	100	1	100	100	100
Gala	97.1	2	100	100	100
Pink lady	97.1	2	100	100	100
Overall	99	3	100	100	100

282 By comparing the above results, many classifiers on image data achieves the same level of accuracies  
 283 compared to PLS-DA on spectral data when classifying apples from Braeburn and Gala variety. If we merge  
 284 the apples of different varieties, the best classification result of image data will be lower than that of spectral  
 285 data by 6.7%. Such degradation in performance indicates that the image data has lower quality compared to  
 286 the spectral one. However, the sensor system is still feasible for organic apple authentication ( $\geq 90\%$  accuracy)  
 287 with the aid of state of the art machine learning methods.

288 **4. Conclusion**

289 A prototype sensor system and ten classification methods were evaluated as a solution for fast and non-  
290 destructive detection of apple quality, more specifically, to determine if an apple is organic or conventional.  
291 The rainbow image data obtained from the sensor system was lower in resolution and higher in degree of  
292 nonlinearity compared to the spectral data generated by a commercial spectrometer. It was found that the  
293 classification results of image data were comparable to that of spectral data when equipped with the of state  
294 of the art classifiers, such as SVM and LW-PLSC. Such results demonstrate the effectiveness and significance  
295 of the sensor system for differentiating organic apples from conventional ones based on the colour level.  
296 Moreover, the sensor system has extremely lower price in hardware compared to commercial spectrometer,  
297 which is practically suitable for low-cost food quality detection. **However, due to the instrumental restrictions**  
298 **(size of diffraction grating sheet, dispersion of flashlight and resolution of smartphone camera), the food**  
299 **produce used for experiments currently requires having a proper size and shape to ensure that a complete**  
300 **rainbow image is clearly presented and effectively captured.** Our future work will optimize the experimental  
301 settings and improve the detection performance by selecting variables of class distinction.

302 **Acknowledgments**

303 This work was supported by Fujian science and technology department project (No. JK2017007), Natural  
304 Science Foundation of Fujian Province, China (No. 2018J01776), Natural Science Foundation of Fujian  
305 Province, China (No. 2018J01775) and the National Natural Science Foundation of China under Grant (No.  
306 61672157).

307 **References**

- 308 Aggarwal, C.C., Hinneburg, A., Keim, D.A., 2001. On the Surprising Behavior of Distance Metrics in High Dimensional Space BT -  
309 Database theory, in: Database Theory. pp. 420–434.
- 310 Ballabio, D., Consonni, V., 2013. Classification tools in chemistry. Part 1: Linear models. PLS-DA. Anal. Methods 5, 3790–3798.  
311 <https://doi.org/10.1039/c3ay40582f>
- 312 Barker, M., Rayens, W., 2003. Partial least squares for discrimination. J. Chemom. 17, 166–173. <https://doi.org/10.1002/cem.785>

313 Cárdenas-Pérez, S., Chanona-Pérez, J., Méndez-Méndez, J. V., Calderón-Domínguez, G., López-Santiago, R., Perea-Flores, M.J.,  
314 Arzate-Vázquez, I., 2017. Evaluation of the ripening stages of apple (Golden Delicious) by means of computer vision system.  
315 *Biosyst. Eng.* 159, 46–58. <https://doi.org/10.1016/j.biosystemseng.2017.04.009>

316 Chang, C.C., Lin, C.J., 2011. LIBSVM: A Library for support vector machines. *ACM Trans. Intell. Syst. Technol.*  
317 <https://doi.org/10.1145/1961189.1961199>

318 Cruz-Fernández, M., Luque-Cobija, M.J., Cervera, M.L., Morales-Rubio, A., de la Guardia, M., 2017. Smartphone determination of fat  
319 in cured meat products. *Microchem. J.* <https://doi.org/10.1016/j.microc.2016.12.020>

320 Cubero, S., Albert, F., Prats-Moltalbán, J.M., Fernández-Pacheco, D.G., Blasco, J., Aleixos, N., 2018. Application for the estimation of  
321 the standard citrus colour index (CCI) using image processing in mobile devices. *Biosyst. Eng.* 167, 63–74.  
322 <https://doi.org/10.1016/j.biosystemseng.2017.12.012>

323 De Brabanter, K., Karsmakers, P., Ojeda, F., Alzate, C., De Brabanter, J., Pelckmans, K., De Moor, B., Vandewalle, J., Suykens, J.,  
324 2011. *LS-SVMLab Toolbox User's Guide Version 1.8*. ESAT-SISTA Tech. Rep.

325 de Lima, M.D., Barbosa, R., 2019. Methods of Authentication of Food Grown in Organic and Conventional Systems Using  
326 Chemometrics and Data Mining Algorithms: a Review. *Food Anal. Methods* 887–901. [https://doi.org/10.1007/s12161-018-](https://doi.org/10.1007/s12161-018-01413-3)  
327 [01413-3](https://doi.org/10.1007/s12161-018-01413-3)

328 Despagne, F., Luc Massart, D., Chabot, P., 2000. Development of a robust calibration model for nonlinear in-line process data. *Anal.*  
329 *Chem.* 72, 1657–1665. <https://doi.org/10.1021/ac991076k>

330 Devos, O., Ruckebusch, C., Durand, A., Duponchel, L., Huvenne, J.P., 2009. Support vector machines (SVM) in near infrared (NIR)  
331 spectroscopy: Focus on parameters optimization and model interpretation. *Chemom. Intell. Lab. Syst.* 96, 27–33.  
332 <https://doi.org/10.1016/j.chemolab.2008.11.005>

333 Dhakal, S., Li, Y., Peng, Y., Chao, K., Qin, J., Guo, L., 2014. Prototype instrument development for non-destructive detection of  
334 pesticide residue in apple surface using Raman technology. *J. Food Eng.* 123, 94–103.  
335 <https://doi.org/10.1016/j.jfoodeng.2013.09.025>

336 Dong, J., Guo, W., 2015. Nondestructive Determination of Apple Internal Qualities Using Near-Infrared Hyperspectral Reflectance  
337 Imaging. *Food Anal. Methods* 8, 2635–2646. <https://doi.org/10.1007/s12161-015-0169-8>

338 Dubey, S.R., Jalal, A.S., 2016. Apple disease classification using color, texture and shape features from images. *Signal, Image Video*  
339 *Process.* 10, 819–826. <https://doi.org/10.1007/s11760-015-0821-1>

340 Fan, Y., Lai, K., Rasco, B.A., Huang, Y., 2015. Determination of carbaryl pesticide in Fuji apples using surface-enhanced Raman  
341 spectroscopy coupled with multivariate analysis. *LWT - Food Sci. Technol.* 60, 352–357.  
342 <https://doi.org/10.1016/j.lwt.2014.08.011>

343 Gao, F., Dong, Y., Xiao, W., Yin, B., Yan, C., He, S., 2016. LED-induced fluorescence spectroscopy technique for apple freshness and



344 quality detection. *Postharvest Biol. Technol.* 119, 27–32. <https://doi.org/10.1016/j.postharvbio.2016.04.020>

345 Ignat, T., Lurie, S., Nyasordzi, J., Ostrovsky, V., Egozi, H., Hoffman, A., Friedman, H., Weksler, A., Schmilovitch, Z., 2014. Forecast  
346 of Apple Internal Quality Indices at Harvest and During Storage by VIS-NIR Spectroscopy. *Food Bioprocess Technol.* 7, 2951–  
347 2961. <https://doi.org/10.1007/s11947-014-1297-7>

348 Jarolmasjed, S., Zúñiga Espinoza, C., Sankaran, S., 2017. Near infrared spectroscopy to predict bitter pit development in different  
349 varieties of apples. *J. Food Meas. Charact.* 11, 987–993. <https://doi.org/10.1007/s11694-017-9473-x>

350 Jha, S.N., Ruchi, G., 2010. Non-destructive prediction of quality of intact apple using near infrared spectroscopy. *J. Food Sci. Technol.*  
351 47, 207–213. <https://doi.org/10.1007/s13197-010-0033-1>

352 Jiang, N., Song, W., Wang, H., Guo, G., Liu, Y., 2018. Differentiation between organic and non-organic apples using diffraction grating  
353 and image processing—A cost-effective approach. *Sensors (Switzerland)* 18, 1667. <https://doi.org/10.3390/s18061667>

354 Kim, S., Kano, M., Nakagawa, H., Hasebe, S., 2011. Estimation of active pharmaceutical ingredients content using locally weighted  
355 partial least squares and statistical wavelength selection. *Int. J. Pharm.* 421, 269–274.  
356 <https://doi.org/10.1016/j.ijpharm.2011.10.007>

357 Liu, N., Parra, H.A., Pustjens, A., Hettinga, K., Mongondry, P., van Ruth, S.M., 2018. Evaluation of portable near-infrared spectroscopy  
358 for organic milk authentication. *Talanta* 184, 128–135. <https://doi.org/10.1016/j.talanta.2018.02.097>

359 Luo, H., Huang, Y., Lai, K., Rasco, B.A., Fan, Y., 2016. Surface-enhanced Raman spectroscopy coupled with gold nanoparticles for  
360 rapid detection of phosmet and thiabendazole residues in apples. *Food Control* 68, 229–235.  
361 <https://doi.org/10.1016/j.foodcont.2016.04.003>

362 Luo, W., Huan, S., Fu, H., Wen, G., Cheng, H., Zhou, J., Wu, H., Shen, G., Yu, R., 2011. Preliminary study on the application of near  
363 infrared spectroscopy and pattern recognition methods to classify different types of apple samples. *Food Chem.* 128, 555–561.  
364 <https://doi.org/10.1016/j.foodchem.2011.03.065>

365 Ma, F., Dong, D., 2014. A Measurement Method on Pesticide Residues of Apple Surface Based on Laser-Induced Breakdown  
366 Spectroscopy. *Food Anal. Methods* 7, 1858–1865. <https://doi.org/10.1007/s12161-014-9828-4>

367 Ma, T., Li, X., Inagaki, T., Yang, H., Tsuchikawa, S., 2018. Noncontact evaluation of soluble solids content in apples by near-infrared  
368 hyperspectral imaging. *J. Food Eng.* 224, 53–61. <https://doi.org/10.1016/j.jfoodeng.2017.12.028>

369 Moncayo, S., Manzoor, S., Navarro-Villoslada, F., Caceres, J.O., 2015. Evaluation of supervised chemometric methods for sample  
370 classification by Laser Induced Breakdown Spectroscopy. *Chemom. Intell. Lab. Syst.* 146, 354–364.  
371 <https://doi.org/10.1016/j.chemolab.2015.06.004>

372 Moscetti, R., Raponi, F., Ferri, S., Colantoni, A., Monarca, D., Massantini, R., 2018. Real-time monitoring of organic apple (var. Gala)  
373 during hot-air drying using near-infrared spectroscopy. *J. Food Eng.* 222, 139–150.  
374 <https://doi.org/10.1016/j.jfoodeng.2017.11.023>

375 Otsu, N., 1979. A Threshold Selection Method from Gray-Level Histograms. *IEEE Trans. Syst. Man. Cybern.* 9, 62–66.  
376 <https://doi.org/10.1109/TSMC.1979.4310076>

377 Snee, R.D., 1977. Validation of Regression Models: Methods and Examples. *Technometrics* 19, 415–428.  
378 <https://doi.org/10.1080/00401706.1977.10489581>

379 Song, W., Wang, H., Maguire, P., Nibouche, O., 2018a. Nearest clusters based partial least squares discriminant analysis for the  
380 classification of spectral data. *Anal. Chim. Acta* 1009, 27–38. <https://doi.org/10.1016/j.aca.2018.01.023>

381 Song, W., Wang, H., Maguire, P., Nibouche, O., 2018b. Collaborative representation based classifier with partial least squares regression  
382 for the classification of spectral data. *Chemom. Intell. Lab. Syst.* 182, 79–86. <https://doi.org/10.1016/j.chemolab.2018.08.011>

383 Song, W., Wang, H., Maguire, P., Nibouche, O., 2016. Differentiation of organic and non-organic apples using near infrared reflectance  
384 spectroscopy — A pattern recognition approach. *2016 IEEE Sensors* 1–3. <https://doi.org/10.1109/ICSENS.2016.7808530>

385 Strobl, C., Malley, J., Tutz, G., 2009. An Introduction to Recursive Partitioning: Rationale, Application, and Characteristics of  
386 Classification and Regression Trees, Bagging, and Random Forests. *Psychol. Methods* 14, 323–348.  
387 <https://doi.org/10.1037/a0016973>

388 Sun, K., Li, Y., Peng, J., Tu, K., Pan, L., 2017. Surface Gloss Evaluation of Apples Based on Computer Vision and Support Vector  
389 Machine Method. *Food Anal. Methods* 10, 2800–2806. <https://doi.org/10.1007/s12161-017-0849-7>

390 Suykens, J.A.K., Vandewalle, J., 1999. Least Squares Support Vector Machine Classifiers. *Neural Process. Lett.* 9, 293–300.  
391 <https://doi.org/10.1023/A:1018628609742>

392 Tan, W., Sun, L., Yang, F., Che, W., Ye, D., Zhang, D., Zou, B., 2018. Study on bruising degree classification of apples using  
393 hyperspectral imaging and GS-SVM. *Optik (Stuttg.)* 154, 581–592. <https://doi.org/10.1016/j.ijleo.2017.10.090>

394 Tang, C., He, H., Li, E., Li, H., 2018. Multispectral imaging for predicting sugar content of ‘Fuji’ apples. *Opt. Laser Technol.* 106, 280–  
395 285. <https://doi.org/10.1016/j.optlastec.2018.04.017>

396 Vetrekar, N.T., Gad, R.S., Fernandes, I., Parab, J.S., Desai, A.R., Pawar, J.D., Naik, G.M., Umopathy, S., 2015. Non-invasive  
397 hyperspectral imaging approach for fruit quality control application and classification: case study of apple, chikoo, guava fruits.  
398 *J. Food Sci. Technol.* 52, 6978–6989. <https://doi.org/10.1007/s13197-015-1838-8>

399 Xiao, G., Dong, D., Liao, T., Li, Y., Zheng, L., Zhang, D., Zhao, C., 2015. Detection of Pesticide (Chlorpyrifos) Residues on Fruit Peels  
400 Through Spectra of Volatiles by FTIR. *Food Anal. Methods* 8, 1341–1346. <https://doi.org/10.1007/s12161-014-0015-4>

401 Yuan, L. ming, Cai, J. rong, Sun, L., Han, E., Ernest, T., 2016. Nondestructive Measurement of Soluble Solids Content in Apples by a  
402 Portable Fruit Analyzer. *Food Anal. Methods* 9, 785–794. <https://doi.org/10.1007/s12161-015-0251-2>

403 Zhang, B., Huang, W., Gong, L., Li, J., Zhao, C., Liu, C., Huang, D., 2015. Computer vision detection of defective apples using  
404 automatic lightness correction and weighted RVM classifier. *J. Food Eng.* 146, 143–151.

405 <https://doi.org/10.1016/j.jfoodeng.2014.08.024>

406 Zhang, T., Xia, D., Tang, H., Yang, X., Li, H., 2016. Classification of steel samples by laser-induced breakdown spectroscopy and  
407 random forest. *Chemom. Intell. Lab. Syst.* 157, 196–201. <https://doi.org/10.1016/j.chemolab.2016.07.001>

408 Zheng, W., Fu, X., Ying, Y., 2014. Spectroscopy-based food classification with extreme learning machine. *Chemom. Intell. Lab. Syst.*  
409 139, 42–47. <https://doi.org/10.1016/j.chemolab.2014.09.015>

410 Zou, H.Y., Wu, H.L., Fu, H.Y., Tang, L.J., Xu, L., Nie, J.F., Yu, R.Q., 2010. Variable-weighted least-squares support vector machine  
411 for multivariate spectral analysis. *Talanta* 80, 1698–1701. <https://doi.org/10.1016/j.talanta.2009.10.009>

412

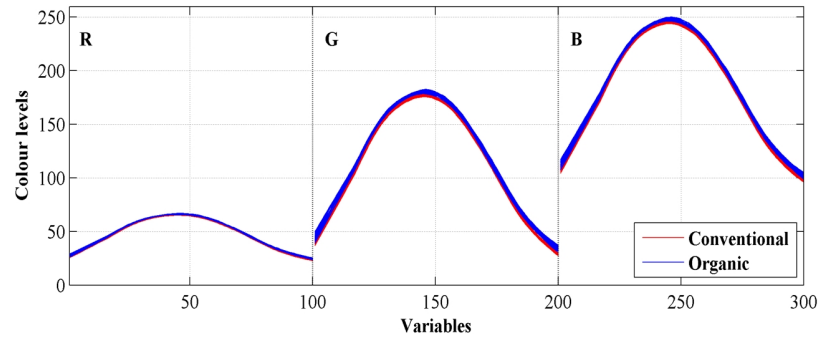
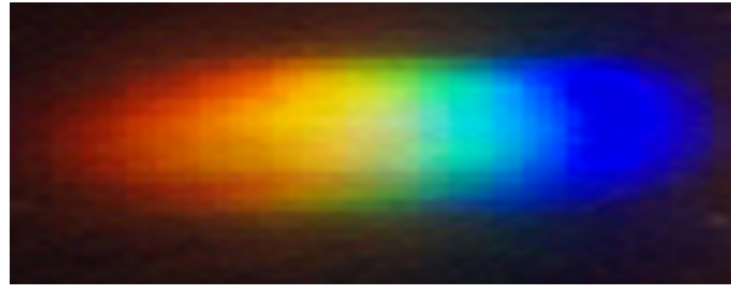
## HIGHLIGHTS

- A low-cost sensor system was used to differentiate organic apples from conventional ones.
- Ten machine learning algorithms were evaluated using rainbow image data from the sensor system.
- The classification results of rainbow image data were comparable to that of spectral data.

**Conventional and organic apples**



**Rainbow image data**



**Classification**

